Progress In Electromagnetics Research C, Vol. 2, 127–158, 2008

PERFORMANCE ANALYSIS OF OS STRUCTURE OF CFAR DETECTORS IN FLUCTUATING TARGET ENVIRONMENTS

M. B. El Mashade

Electrical Engineering Dept., Faculty of Engineering
Al Azhar University
Nasr City, Cairo, Egypt

Abstract—This paper is intended to the analysis of adaptive radar detectors for partially correlated χ^2 targets. This important class of targets is represented by the so-called moderately fluctuating Rayleigh targets, which, when illuminated by a coherent pulse train, return a train of correlated pulses with a correlation coefficient in the range $0 < \rho < 1$ (intermediate between SWII and SWI models). The detection of this type of fluctuating targets is practically of great importance. Since the CFAR detectors represent an attractive class of schemes that can be used to overcome the problem of clutter by adaptively setting their threshold based on local information of total noise power, they are commonly used to decide the presence or absence of the radar target of interest, which is of partially correlated χ^2 type. In addition, the OS based algorithms are chosen to carry out this task owing to their immunity to outlying targets which may be present amongst the contents of the reference window. Moreover, since the large processing time of the single-window OS detector limits its practical applications, our scope here is to analyze the performance of OS modified versions for moderately fluctuating Rayleigh targets in nonideal situations. This analysis includes the single-window as well as the double-window OS detection schemes for the case where the radar receiver postdetection integrates M square-law detected pulses and the signal fluctuation obeys χ^2 statistics with two degrees of freedom. These detectors include the mean-level (ML-), the maximum (MX-) and the minimum (MN-) OS algorithms. Exact formulas for their detection probabilities are derived, in the absence as well as in the presence of spurious targets. The primary and the secondary interfering targets are assumed to be of the moderately fluctuating Rayleigh targets. Swerling's well known cases I and II represent the cases where the signal is completely correlated and completely decorrelated, respectively, from pulse to

pulse. Under the multiple-target operations, the ML-OS detector has the best homogeneous performance, the MN processor has the best multitarget performance when a cluster of radar targets appears in the reference window, while the MX scheme doesn't offer any excessive merits, neither in the absence nor in the presence of outlying targets, as expected.

1. INTRODUCTION

The returned signal from radar target is usually buried in thermal noise and clutter. Since neither the clutter power nor the noise power is known at any given location, a fixed threshold detection processor cannot be applied if the false alarm rate is desired to be controlled. Therefore, it is necessary for automatic detection radars to be adaptive to variations in background clutter in order to achieve the CFAR property. The CFAR detector is one of the most important parts of modern radar signal processing. It can be used to avoid computer overloading, which is caused by radar clutter fluctuation, and obtain high detection performance. This detector employs an adaptive threshold in order to maintain a constant rate of false alarm, irrespective to clutter power, and to maximize the detection performance [1–3]. The CFAR system makes use of the fact that the amplitude variation of weather and sea clutter has a Rayleigh distribution, and is capable of reducing the clutter output to about the same level as the receiver noise level. There are three general CFAR processing approaches: the adaptive threshold CFAR processor, the nonparametric CFAR processor, and the nonlinear receiver. The adaptive threshold CFAR assumes that the probability density of the interference is known except for a few unknown parameters. The unknown parameters are estimated on a cell-by-cell basis by examining reference cells surrounding the cell under test. The resulting probability density function is then used in each cell to obtain a threshold setting that provides the desired false alarm rate. The nonparametric processor, on the other hand, provides CFAR performance for a wide class of input noise distributions [4]. This processor assumes that the statistics of the interference are unknown and transforms this unknown density into a known density where a fixed threshold produces the CFAR action. The nonparametric processors generally exhibit a substantial CFAR loss. Moreover, although nonparametric methods have advantages of implementation, they result in a detector performance that is inferior to that of optimum parametric detectors that have been designed to operate

under conditions in which the signal and noise statistics are known. Nonlinear receivers attempt to control the processor gain as a function of the interference level to provide the desired CFAR action. In general, nonlinear receivers exhibit a large CFAR loss.

The most conventional CFAR schemes are of the mean-level type such as the cell-averaging (CA) and its modified versions [1–3, 7, 15, 16]. The CA-CFAR detector uses the maximum likelihood estimate of the noise power to set the threshold adaptively on the assumption that the underlying noise distribution is exponential and the noise samples are independent and identically distributed (IID). Unfortunately, its detection performance degrades considerably in nonhomogeneous situations caused by multiple targets and clutter edges. The CA processor turns out to perform very poorly in these situations, and if some resilience against interferers and/or clutter edges is to be gained, alternative schemes, must be adopted.

Greater robustness has been obtained with the data censoring algorithms. These systems rely on ordering or ranking the samples in the reference window and take an appropriate reference cell to estimate the background clutter power level. This allows censoring of a certain number of outliers, and consequently the censoring schemes perform creditably as long as the number of interfering targets does not exceed the number of top ranked censored samples. The ordered-statistic (OS) detector has small additional detection loss over the CA-CFAR detector in uniform noise background and can resolve closely spaced targets [5, 7]. However, the large processing time required by this technique limits its practical use. To reduce this processing time in half, the modified versions of this processor have been suggested. They have been proposed by Elias-Fuste [8], and analyzed by You [10], and El Mashade [11] for their performance evaluation in the single sweep case. Noncoherent integration analysis of these processors is carried out in [9] for their performance evaluation in homogeneous background, and their nonhomogeneous performance has been analyzed by El Mashade [14]. Finally, El Mashade [13] analyzed their M-correlated sweeps in nonhomogeneous situations.

It is often assumed that the Swerling cases bracket the behavior of fluctuating targets of practical interest. However, recent investigations of target cross section fluctuation statistics indicate that some targets may have probability of detection curves which lie considerably outside the range of cases which are satisfactorily bracketed by the Swerling cases. An important class of targets is represented by the so-called moderately fluctuating Rayleigh targets, which, when illuminated by a coherent pulse train, return a train of correlated pulses with a correlation coefficient in the range $0 < \rho < 1$ (intermediate between

SWII & SWI models). The detection of this type of fluctuating targets is of great importance. In order that our previous work [14] be sufficiently general to be applicable to a variety of cases, our goal in the present paper is to analyze the performance of the OS based detectors for partially correlated χ^2 targets with two degrees of freedom in the absence as well as in the presence of spurious targets. The χ^2 target model includes the well known SWI and SWII models as special cases. In section II, we formulate the problem and compute the moment generating function of the postdetection integrator output for the case where the signal fluctuation obeys χ^2 statistics with two degrees of freedom that is considered for the study of the signal processing algorithms. The performance of the schemes under consideration is analyzed in Section 3 and their performance is assessed in Section 4. In Section 5, we present a brief discussion along with our conclusions.

2. BACKGROUND AND PROBLEM FORMULATION

The block diagram of typical CFAR processor with postdetection integration of M pulses is shown in Fig. 1. Here, we consider a radar system in which time diversity transmission is employed and assume that M pulses hit the target. Suppose that the receiver model is the familiar one [7] with white receiver noise, independent from pulse to pulse; a normalized square-law envelope detector; and uniform integration of M detector outputs followed by an adaptive CFAR detection scheme. The received IF signal is applied to a matched filter, which is specifically designed to maximize the output signal-to-noise ratio. The output of the matched filter is then passed through a square-law device to extract the baseband signal. This signal is then sampled and the sampling rate is assumed to be such that the samples are statistically independent. The square-law detected video range samples are sent serially into a shift register of $N + 1$ resolution cells resulting in a matrix of $M \times (N + 1)$ observations which are denoted by q_{ij}. The M observations from the cell under test, which is the one in the middle of the processing window, are represented by Y. The center bin (test cell) is tested on whether it contains the target or not. The detection procedures involve the comparison of the received signal with a certain threshold. When the background noise power fluctuates, it is difficult to maintain a constant rate for the false alarm if the detection threshold is fixed. Thus, the CFAR schemes set this threshold adaptively according to local information on the background noise power. The estimation of the mean power of the local clutter (Z) is usually based on the N neighboring bins. The name of the specific CFAR detector is determined according to the kind of operation used

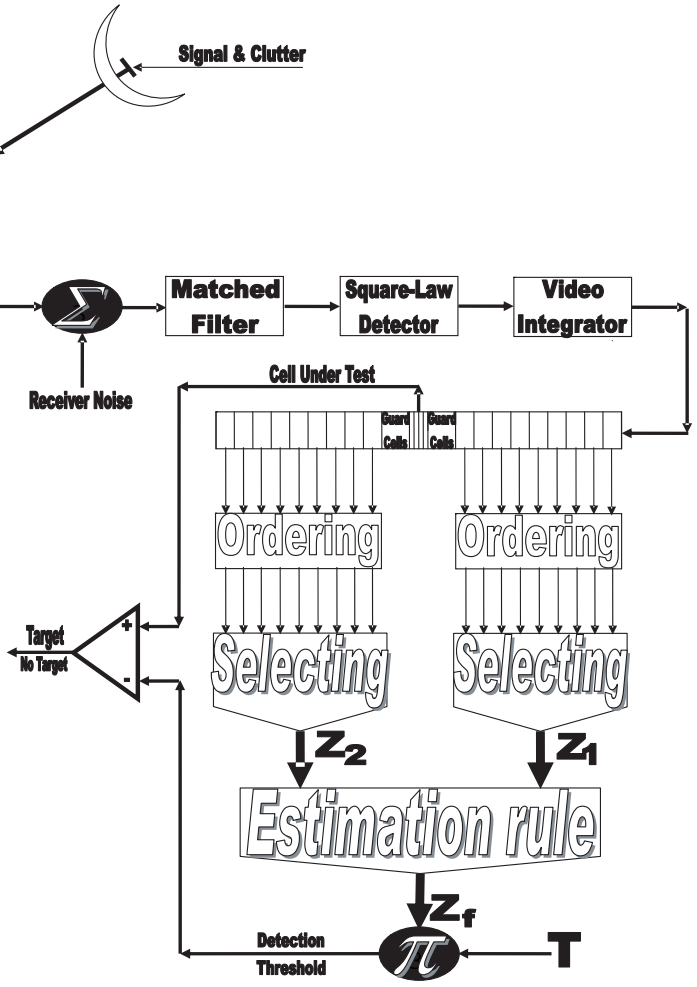

Figure 1. Architecture of OS structure of CFAR detectors with postdetection integration.

to estimate the unknown noise power level. In this manuscript, we are concerned with the CFAR processors in which the ordered-statistic (OS) technique is implemented. The detection problem consists of testing the hypothesis H_0 (absence of signal) versus the alternative H_1 (presence of signal). Precisely, we have

$$y(t) = \begin{cases} n(t) & \text{under} \quad H_0 \\ s(t) + n(t) & \text{under} \quad H_1 \end{cases} \qquad t \in [0, T_0] \tag{1}$$

$[0, T_0]$ represents the observation interval, $s(t)$ and $n(t)$ denote the baseband equivalents of received waveform and noise, respectively.

In order to analyze the detection performance of a CFAR processor, let the input to the square-law detector consists of M pulses, each composed of a steady signal component and Gaussian noise. Denote the in phase and quadrature components of the signal over the M pulses by the $M \times 1$ vectors S_i and S_q, respectively, and denote the in phase and quadrature components of the noise by $M \times 1$ vectors N_i and N_q, respectively. Then, the integrated output of the square-law detector is

$$Y \underline{\Delta} \ |S_i + N_i|^2 + |S_q + N_q|^2 \tag{2}$$

The moment generating function (MGF) associated with the random variable (RV) Y is defined as

$$M_Y(\omega) \underline{\Delta} \int_{-\infty}^{\infty} f_Y(x) \exp(-\omega x) \ dx \tag{3}$$

In the above expression, $f_Y(.)$ denotes the probability density function (PDF) of Y. Substituting Eq. (2) for the random variable Y, Eq. (3) takes the form

$$M_Y(\omega) = \int_{-\infty}^{\infty} \int_{-\infty}^{\infty} f(N_i, N_q) \exp\left(-\omega \left(|S_i + N_i|^2 + |S_q + N_q|^2\right)\right) dN_i dN_q \tag{4}$$

If N_i and N_q are Gaussian and IID random vectors, one may write

$$f(N_i, N_q) = \left(\frac{1}{2\pi\sigma^2}\right)^M \exp\left(-\frac{|N_i|^2 + |N_q|^2}{2\sigma^2}\right) \tag{5}$$

The substitution of Eq. (5) into Eq. (4) yields

$$\begin{aligned} M_Y(\omega) \ = \ & \left(\frac{1}{2\pi\sigma^2}\right)^M \int_{-\infty}^{\infty} \int_{-\infty}^{\infty} \exp\left(-\frac{|N_i|^2 + 2\omega\sigma^2 |S_i + N_i|^2}{2\sigma^2}\right) \\ & \times \exp\left(-\frac{|N_q|^2 + 2\omega\sigma^2 |S_q + N_q|^2}{2\sigma^2}\right) dN_i dN_q \end{aligned} \tag{6}$$

Completing the squares in N_i and N_q and integrating over N_i and N_q, one obtains

$$M_Y(\omega) = \left(\frac{1}{1 + 2\omega\sigma^2}\right)^M \exp\left(-\frac{\omega \left(|S_i|^2 + |S_q|^2\right)}{1 + 2\omega\sigma^2}\right) \tag{7}$$

If the signal component fluctuates, then the MGF of the square-law detector is a weighted average, accounting for the PDF of the in phase and quadrature components of the signal. Hence, for a fluctuating target, the MGF of the detector output is [6]

$$\overline{M}_Y(\omega) = \int_{-\infty}^{\infty}\int_{-\infty}^{\infty} M_Y(\omega) f_{S_i}(S_i) f_{S_q}(S_q)\, dS_i dS_q \tag{8}$$

Assuming that S_i and S_q are IID with PDF $S(x)$, we have

$$\overline{M}_Y(\omega) = \left(\frac{1}{1+2\omega\sigma^2}\right)^M \left\{\int_{-\infty}^{\infty} f_S(X) \exp\left(-\frac{\omega|X|^2}{1+2\omega\sigma^2}\right) dX\right\}^2 \tag{9}$$

Using Eq. (9), one may compute the MGF for any target PDF.

2.1. Correlated χ^2 Signal Model

Most radar targets are complex objects and produce a wide variety of reflections. Different targets often require different models to characterize the varied statistical nature of these responses. A radar target whose return varies up and down in amplitude as a function of time is known as fluctuating target. The fluctuation rate may vary from essentially independent return amplitudes from pulse-to-pulse to significant variation only on a scan-to-scan basis. The χ^2 family is one of the most radar cross-section fluctuation models. The χ^2 distribution with $2\,K$ degrees of freedom has a PDF given by

$$f_S(\sigma) = \frac{1}{\Gamma(K)}\left(\frac{K}{\overline{\sigma}}\right)^K \sigma^{K-1} \exp\left(-\frac{K}{\overline{\sigma}}\sigma\right) U(\sigma) \tag{10}$$

In the above expression, $\overline{\sigma}$ is the average cross section over all target fluctuations and $U(.)$ denotes the unit step function. When $K = 1$, the PDF of Eq. (10) reduces to the exponential or Rayleigh power distribution that applies to the Swerling cases I and II.

The above formula represents the PDF of the sum of the squares of $2K$ real Gaussian RV's or the sum of the squared magnitudes of K complex Gaussian RV's. Therefore, if $K = 1$, then σ may be generated as $\sigma = x_1^2 + x_2^2$, where $x_i,\ i = 1, 2$, are IID Gaussian RV's, each with zero mean and $\overline{\sigma}/2$ variance. The magnitude of the in phase component is $u = x_1$. If $\alpha = \overline{\sigma}/2$, we can write the PDF of u as

$$f_u(x_1) = \frac{1}{\sqrt{2\pi\alpha}} \exp\left(-\frac{x_1^2}{2\alpha}\right) \tag{11}$$

To accommodate an $M \times 1$ vector of correlated χ^2 RV's with two degrees of freedom, we introduce the PDF of the M-dimensional vector X_1

$$f_{X_1}(X) = \left(\frac{1}{2\pi\alpha}\right)^{\frac{M}{2}} \frac{1}{\sqrt{|\Lambda|}} \exp\left(-\frac{X^T \Lambda^{-1} X}{2\alpha}\right) \tag{12}$$

In the above expression, Λ represents the correlation matrix of $x_{11}, x_{12}, \ldots, x_{1M}$ and T denotes the vector transpose. The substitution of Eq. (12) into Eq. (9) yields

$$\overline{M}_Y(\omega) = \left(\frac{1}{1+2\omega\sigma^2}\right)^M \left\{\int_{-\infty}^{\infty} \left(\frac{1}{2\pi\alpha}\right)^{\frac{M}{2}} \frac{1}{\sqrt{|\Lambda|}} \exp\left(-\frac{1}{2\alpha} X^T \left(\Lambda^{-1} + \frac{2\omega\alpha}{1+2\omega\sigma^2} I\right) X\right) dX\right\}^2 \tag{13}$$

I denotes the identity matrix. Carrying the above integration leads to

$$\overline{M}_Y(\omega) = \frac{1}{|(1+2\omega\sigma^2)I + 2\omega\alpha\Lambda|} \tag{14}$$

Expressing the determinant in terms of the nonnegative eigenvalues $\lambda_1, \lambda_2, \ldots, \lambda_M$ of Λ, Eq. (14) takes the form

$$\overline{M}_Y(\omega) = \prod_{i=1}^{M} \frac{1}{1+2\omega(\sigma^2+\alpha\lambda_i)} = \prod_{i=1}^{M} \frac{1}{1+\psi(1+A\lambda_i)\omega} \tag{15}$$

$\psi = 2\sigma^2$ represents the noise power and $A = 2\alpha/\psi$ is the average signal-to-noise ratio (SNR). It is important to note that $\overline{M}_Y(\omega)$ is the Laplace transformation of the PDF of the sum of M square-law detected pulses of a χ^2 ($K = 1$) signal in Gaussian noise.

The Swerling case I (slow fluctuation) model is represented by choosing $\lambda_1 = M,\ \lambda_i = 0$ for $2 \le i \le M$. Thus, for SWI, we have

$$\overline{M}_Y(\omega) = \frac{1}{1+\psi(1+MA)\omega} \left(\frac{1}{1+\psi\omega}\right)^{M-1} \quad \text{for SWI model} \tag{16}$$

which agrees with Swerling's result [12]. The fast fluctuation (SWII), on the other hand, can be represented by choosing $\lambda_i = 1$ for $1 \le i \le M$, which yields

$$\overline{M}_Y(\omega) = \left(\frac{1}{1+\psi(1+A)\omega}\right)^M \quad \text{for SWI model} \tag{17}$$

In view of Eq. (15), the solution for the partially correlated case requires computation of the eigenvalues of the correlation matrix Λ. It is assumed here that: i) The statistics of the signal are stationary, and ii) The signal can be represented by a first order Markov process. Under these assumptions, Λ is a Toeplitz nonnegative definite matrix of the following general form:

$$\Lambda = \begin{bmatrix} 1 & \rho & \rho^2 & \cdot & \cdot & \cdot & \rho^{M-2} & \rho^{M-1} \\ \rho & 1 & \rho & \cdot & \cdot & \cdot & \rho^{M-3} & \rho^{M-2} \\ \rho^2 & \rho & 1 & \cdot & \cdot & \cdot & \rho^{M-4} & \rho^{M-3} \\ \cdot & \cdot & \cdot & \cdot & \cdot & \cdot & \cdot & \cdot \\ \cdot & \cdot & \cdot & \cdot & \cdot & \cdot & \cdot & \cdot \\ \cdot & \cdot & \cdot & \cdot & \cdot & \cdot & \cdot & \cdot \\ \rho^{M-2} & \rho^{M-3} & \rho^{M-4} & \cdot & \cdot & \cdot & 1 & \rho \\ \rho^{M-1} & \rho^{M-2} & \rho^{M-3} & \cdot & \cdot & \cdot & \rho & 1 \end{bmatrix} \quad 0 \leq \rho \leq 1 \tag{18}$$

Eqs. (15)–(18) are the basic formulas of our analysis in this paper.

The PDF of the output of the ith test tap is given by the Laplace inverse of Eq. (15) after making some minor modifications. If the ith test tap contains noise alone, we let $A = 0$, that is the average noise power at the receiver input is ψ. If the ith range cell contains a return from the primary target, it rests as it is without any modifications, where A represents the strength of the target return at the receiver input. On the other hand, if the ith test observation is corrupted by interfering target return, A must be replaced by I, where I denotes the interference-to-noise (INR) at the receiver input.

3. PROCESSOR PERFORMANCE EVALUATION IN MULTITARGET SITUATIONS

CFAR procedures were originally developed using a statistical model of uniform background noise. However, this is not representative of real situations. It is impossible to describe all radar working conditions by a single model, yet consideration of a larger number of different situations might be confusing. For these reasons, three different signal situations are selected: uniform clutter, clutter edges and multiple targets. Each one of these situations is represented by a distinct signal model. The different CFAR schemes are investigated and compared on the background of these three signal cases. A uniform clutter model describes the classical situation with stationary noise in the reference window. Clutter edges, on the other hand, are used to

describe transition areas between regions with very different noise characteristics. Multiple target situations occur occasionally in radar signal processing when two or more targets are at a very similar range. The consequent masking of one target by the others is called suppression. These interferers can arise from either real object returns or pulsed noise jamming. From a statistical point of view, this implies that the reference samples, although still independent of one another, are no longer identically distributed. In our analysis and study of the nonhomogeneous background for which the reference cells don't follow a single common PDF, we are concerned only with increases in the value of ψ for some isolated reference cells due to the presence of secondary targets. The amplitudes of all the targets present amongst the candidates of the reference window are assumed to be of the same strength and to fluctuate in accordance with the partially correlated χ^2 fluctuation model with correlation coefficient ρ_i. The interference-to-noise ratio (INR) for each of the spurious targets is taken as a common parameter and is denoted by I. Thus, for reference cells containing extraneous target returns, the total background noise power is $\psi(1+I)$, while the remaining reference cells have identical noise power of ψ value.

The ordered-statistic (OS) CFAR detector uses the Kth smallest sample to estimate the total noise power. We will denote by OS(K) the OS scheme with parameter K. The value of K is generally chosen so that the detection probability (in homogeneous background) is maximized. The large processing time taken by this detector in ordering the candidates of the reference window limits its practical uses. Modified versions of this processor have been proposed to solve this problem [8]. Such detectors are specifically tailored to provide good estimates of the noise power as the conventional OS detector. In this section, we analyze the conventional OS scheme as well as three of its modified versions, namely ML-, MX-, and MN-OS schemes, for their performance evaluation in multitarget environment and obtain closed form expression for their detection performances.

3.1. Single-Window OS Detector

The amplitude values taken from the reference window, of size N, are first rank-ordered according to increasing magnitude. The sequence thus achieved is

$$q_{(1)} \leq q_{(2)} \leq q_{(3)} \leq \cdots \leq q_{(K)} \leq \cdots \leq q_{(N)} \tag{19}$$

The indices in parentheses indicate the rank-order number. $q_{(1)}$ denotes the minimum and $q_{(N)}$ the maximum value. The sequence given in

Eq. (19) is called an ordered-statistic. The central idea of an ordered statistic CFAR processor is to select one certain value from the above sequence and to use it as an estimate Z for the average clutter power as observed in the reference window. Thus,

$$Z_{OS} = q_{(K)}, \qquad K \in \{1, 2, 3, \ldots, N\} \tag{20}$$

In the CFAR system, target decision is commonly performed by multiplying this estimation Z_{OS} by a scaling factor T, which is dependent on the applied estimation technique and the required rate of false alarm. The resulting product $Z_{OS}T$ is directly used as the threshold value with which the content of the cell under test Y is compared to decide whether the target is present or absent. A target is declared to be present if Y exceeds the threshold TZ_{OS}. The threshold coefficient T is used to achieve a desired false alarm rate for a given window size N when the total background noise is homogeneous. Since the unknown noise power level estimate Z is a random variable, the processor performance is determined by calculating the average values of false alarm and detection probabilities. The false alarm probability P_{fa} is defined as

$$P_{fa} \triangleq E_z\{P(Y\rangle ZT|H_0)\} = 1 - E_z\{F_Y(ZT)\} \tag{21}$$

In the above expression, $E_Z(.)$ denotes the expectation operator and $F_Y(.)$ represents the cumulative distribution function (CDF) of the random variable Y. When the background clutter is homogeneous, Y has a MGF given by Eq. (15) after setting A equals to zero.

$$\overline{M}_Y(\omega) = \left(\frac{1}{1+\psi\omega}\right)^M \tag{22}$$

The Laplace inverse of Eq. (22) gives the PDF of Y under the null hypothesis (H_0). Thus,

$$f_Y(y|H_0) = \left(\frac{1}{\psi}\right)^M \frac{1}{\Gamma(M)} y^{M-1} \exp\left(-\frac{y}{\psi}\right) U(y) \tag{23}$$

Once the PDF of Y is obtained, we can calculate its associated CDF, which is in turn used to compute the probability of false alarm. Finally, P_{fa} takes the form

$$P_{fa} = \sum_{j=0}^{M-1} \left(\frac{T}{\psi}\right)^j \frac{(-1)^j}{\Gamma(j+1)} \frac{d^j}{d\omega^j} \{M_z(\omega)\}_{\omega=\frac{T}{\psi}} \tag{24}$$

In the above formula, $M_Z(.)$ denotes the MGF of the noise level estimate Z. For a CFAR scheme, $M_Z(T/\psi)$ must be independent of ψ. This is indeed true for all the detection schemes considered here. Under the signal present hypothesis H_1, the statistic Y has a MGF given by Eq. (15) which can be put in another simplified form

$$\overline{M}_Y(\omega) = \prod_{j=1}^{M} \frac{a_j}{\omega + a_j} \quad \text{with} \quad a_j \triangleq \frac{1}{\psi(1 + A\lambda_j)} \tag{25}$$

By using the technique of partial fraction method, the PDF of the cell under test variate Y becomes

$$f_Y(y|H_1) = \sum_{i=1}^{M} D_i \exp(-a_i y) U(y) \tag{26}$$

The constants D_i's are defined as

$$D_i \triangleq a_i \prod_{\substack{j=1 \\ j \neq 1}}^{M} \frac{a_j}{a_j - a_i} \tag{27}$$

Once the PDF of the cell under test variate Y is calculated, the execution of its associated CDF is straightforward. Finally, the processor detection performance takes the following analytical form

$$P_d = \sum_{i=1}^{M} \frac{D_i}{a_i} \{M_z(\omega)\}_{\omega = \frac{T}{\psi(1+A\lambda_i)}} \tag{28}$$

In order to analyze the processor performance when the reference window no longer contains radar returns from a homogeneous background, the assumption of statistical independence of the reference cells is retained. Consider the situation where the reference window contains r interfering target returns, each with power level $\psi(1 + I)$, and the remaining $N - r$ samples having thermal noise only with power level ψ. Under these assumptions, the Kth ordered sample, which represents the noise power level estimate in the OS detector, has a CDF given by [14]

$$\begin{aligned} F_K(z; N, r) \; = \; & \sum_{i=K}^{N} \sum_{j=\max(0, i-r)}^{\min(i, N-r)} \binom{N-r}{j} \binom{r}{i-j} \\ & \times [1 - F_t(z)]^{N-r-j} \{F_t(z)\}^j [1 - F_s(z)]^{r-i+j} \{F_s(z)\}^{i-j} \end{aligned} \tag{29}$$

The CDF of the reference cell that contains a spurious target return can be obtained from

$$F_s(z) = L^{-1}\left\{\frac{1}{\omega}\prod_{\ell=1}^{M}\frac{1}{1+\psi(1+I\lambda_\ell)\omega}\right\} = 1-\sum_{\ell=1}^{M} b_\ell e^{-c_\ell z} \tag{30}$$

where L^{-1} denotes the Laplace inverse operator and

$$b_\ell \triangleq \prod_{\substack{k=1\\k\neq\ell}}^{M}\frac{1+I\lambda_\ell}{I(\lambda_\ell-\lambda_k)} \quad \text{and} \quad c_\ell \triangleq \frac{1}{\psi(1+I\lambda_\ell)} \tag{31}$$

$F_t(.)$ represents the CDF of the reference cell that contains thermal noise only of background power ψ. This CDF is associated with a PDF of a similar form as that given by Eq. (23), which by integrating it we obtain the desired CDF. Thus,

$$F_t(z) = 1-\sum_{j=0}^{M-1}\left(\frac{z}{\psi}\right)^j\frac{1}{\Gamma(j+1)}\exp\left(-\frac{z}{\psi}\right)U(z) \tag{32}$$

The substitution of Eqs. (30) and (32) into Eq. (29) yields

$$\begin{aligned} F_K(z;N,r) \;=\; & \sum_{i=K}^{N}\sum_{j=\max(0,i-r)}^{\min(i,N-r)}\binom{N-r}{j}\binom{r}{i-j} \\ & \times\sum_{k=0}^{j}\sum_{\ell=0}^{i-j}\binom{j}{k}\binom{i-j}{\ell}(-1)^{i-k-\ell} \\ & \times\left\{\sum_{m=0}^{M-1}\frac{\left(\frac{z}{\psi}\right)^m}{\Gamma(m+1)}e^{-\frac{z}{\psi}}\right\}^{N-r-k} * \left\{\sum_{n=1}^{M} b_n e^{-c_n z}\right\}^{r-\ell} \end{aligned} \tag{33}$$

The Laplace transformation of the above equation gives

$$\begin{aligned} \Phi_{F_K}(\omega;N,r) \;=\; & \sum_{i=K}^{N}\sum_{j=\max(0,i-r)}^{\min(i,N-r)}\binom{N-r}{j}\binom{r}{i-j} \\ & \times\sum_{k=0}^{j}\sum_{\ell=0}^{i-j}\binom{j}{k}\binom{i-j}{\ell}(-1)^{i-k-\ell}\sum_{\theta_0=0}^{N-r-k}\sum_{\theta_1=0}^{N-r-k} \end{aligned}$$

$$\cdots \sum_{\theta_{M-1}=0}^{N-r-k} \frac{\Omega(N-r-k;\theta_0,\ldots,\theta_{M-1})}{\prod_{v=0}^{M-1}[\Gamma(v+1)]^{\theta_v}} \left(\frac{1}{\psi}\right)^{\sum_{\eta=0}^{M-1}\eta\theta_\eta}$$
$$\times \sum_{\vartheta_1=0}^{r-\ell}\sum_{\vartheta_2=0}^{r-\ell}\cdots\sum_{\vartheta_M=0}^{r-\ell} \Omega(r-\ell;\vartheta_1,\ldots,\vartheta_M)\prod_{\xi=1}^{M}(b_\xi)^{\vartheta_\xi}$$
$$\times \frac{\Gamma\left(\sum_{\gamma=0}^{M-1}\gamma\theta_\gamma+1\right)}{\left(\omega+\dfrac{N-r-k}{\psi}+\sum_{\zeta+1}^{M}\vartheta_\zeta c_\zeta\right)^{\sum_{\gamma=0}^{M-1}\gamma\theta_\gamma+1}} \tag{34}$$

where

$$\Omega(N-i-1;j_0,\ldots,j_{M-1}) \triangleq \begin{cases} \dfrac{\Gamma(N-i)}{\prod_{\ell=0}^{M-1}\Gamma(j_\ell+1)} & \text{for } \sum_{k=0}^{M-1} j_k = N-i-1 \\ 0 & \text{for } \sum_{k=0}^{M-1} j_k \neq N-i-1 \end{cases} \tag{35}$$

Once the Laplace transformation of the CDF of noise power level estimate is computed, the MGF of the final noise power level is calculated as [11]

$$M_z(\omega) \triangleq \omega\Phi_{F_z}(\omega) \tag{36}$$

and consequently, the processor detection performance can be easily evaluated (see Eq. (28)).

Again, the OS-CFAR processor performance is highly dependent upon the value of K. For example, if a single extraneous target appears in the reference window of appreciable magnitude, it occupies the highest ranked cell with high probability. If K is chosen to be N, the estimate will almost always set the threshold based on the value of interfering target. This increases the overall threshold and may lead to a target miss. If, on the other hand, K is chosen to be less than the maximum value, the OS-CFAR scheme will be influenced only slightly for up to N-K spurious targets.

3.2. Double-Window OS Detector

Although the OS-CFAR detector has some advantages over the cell-averaging detector [7–11], the large processing time taken by this technique in sorting the reference cells limits its practical applications. To alleviate this problem, the double-windows OS procedure has been proposed [8]. Employing two simultaneously specialized processors, one for each set of neighboring cells, it is possible to reduce by half the single-window processing time without altering the estimation of the clutter statistics. On the other hand, if the leading and lagging set of cells are independently ordered and subsequently compared under the maximum or minimum criterion, we will obtain a new random variable with differing statistics from the representative cell of the OS-CFAR algorithm.

Three modified versions of the OS-CFAR technique are analyzed in this subsection: the mean-level (ML-), the maximum (MX-) and the minimum (MN-) ordered statistic procedures. Each one of these modified versions can reduce the single-window OS processing time in half and has the same advantages as the OS detector with only a negligible increment to the CFAR loss.

In addition to aiming at reducing the number of excessive false alarms at clutter edges, the modified ordered-statistic processors may also be used in multiple target situations. Here, we examine the effects of outlying targets on detectability of the cell under test. When the number of these targets is within their allowable range, the effect of spurious targets is manifested in a change in the underlying statistical assumptions. This implies that the candidates of the reference sets, although still independent of one another, are no longer identically distributed.

3.2.1. Mean-Level (ML) OS Detector

Referring to Fig. 1, reference cells are equally partitioned into leading and lagging windows Z_1 and Z_2. The generic operation of the two-windows family of CFAR detectors is to process the cells of each local window separately, and then combining the resulting estimates through a mean-level (ML) operation to obtain the final estimate of the unknown noise power level. The candidates of each local window (of size $N/2$) are separately ordered from smallest to largest and then the K_1th order statistic from the leading subset and the K_2th order statistic from the trailing subset are taken to represent the unknown noise power level estimate of each local window.

$$Z_i = q_{(k_i)}, \quad k_i \in \left\{1, 2, 3, \ldots, \frac{N}{2}\right\}, \quad i = 1 \ \& \ 2 \tag{37}$$

In ML-OS detector, the total noise power is estimated by combining the local noise level estimates through the mean operation. The combiner puts out the noise level estimate Z_{ML} as

$$Z_{ML} = mean(Z_1, Z_2) \tag{38}$$

The rationale for the mean family of CFAR schemes is that by choosing the mean, the optimum CFAR detector in a homogeneous background when the reference cells contain IID observations is achieved. In addition, as the size of the reference window increases, the detection probability approaches that of the optimum detector, which is based on a fixed threshold.

Since the total noise power is estimated by averaging the local estimates of the noise power levels, the MGF of Z_{ML} is simply given by the product of the MGF's of Z_1 and Z_2 [4]. Therefore,

$$M_{Z_{ML}}(\omega) = M_{Z_1}(\omega) M_{Z_2}(\omega) \tag{39}$$

where

$$M_{Z_1}(\omega) = \omega \Phi_{F_{K_1}}(\omega; N_1, r_1) \quad \text{and} \quad M_{Z_2}(\omega) = \omega \Phi_{F_{K_2}}(\omega; N_2, r_2) \tag{40}$$

The MGF's of the noise level estimates are given as a function of the Laplace transformation of their CDF's. These CDF's have the same expression as that given by Eq. (34) after replacing N and r by N_1 and r_1 for the statistic Z_1 and by N_2 and r_2 for the statistic Z_2, respectively. Here, r_1 and r_2 represent the number of interfering target returns amongst the contents of the leading and trailing reference windows, respectively, and $N_1 = N_2 = N/2$. Since the MGF of the final noise power level estimate Z_{ML} is the backbone of the processor false alarm and detection performances, the behavior of the scheme under consideration, in multiple target environments, can be easily obtained.

3.2.2. Maximum (MX)-OS Detector

The comparison of the ML-OS characteristics with those of other CFAR schemes demonstrates the superiority of its detection performance in homogeneous background. Nonetheless, its inferior behavior in other situations calls for another modified CFAR processors. Excessive numbers of false alarms at clutter edges and degradation of detection performance in the presence of a cluster of radar targets are the prime motivations for exploring other CFAR procedures that discriminate between the interference and the primary targets. Two such techniques have been investigated that are modifications of the OS technique. Each of these schemes is capable of

overcoming only one of these problems with additional loss of detection power. The first scheme, which is known as the maximum (MX) procedure, is specifically aimed at reducing the number of excessive false alarms in the presence of abrupt change in the noise power from one level to another. The generic operation of the MX family of CFAR schemes is to process the cells from each local window separately and combining them through a maximum operation. The combiner puts out the final noise level estimate

$$Z_{MX} = \max(Z_1, Z_2) \tag{41}$$

The rationale for the maximum detector is that by choosing the larger of the local noise level estimates, the increase in false alarm probability for test cells near the edges of clutter patches is avoided. In addition, when the OS technique is combined with the maximum operation, we obtain a processor that is also robust to interfering targets.

The MX-OS detector uses the maximum of the two local estimates Z_1 and Z_2 to estimate the background noise power level. The CDF associated with this noise power level estimate is [14]

$$F_{Z_{MX}}(z) = F_{Z_1}(z)\ F_{Z_2}(z) \tag{42}$$

By using the generalized formula of the CDF of the Kth ordered statistic, out of N reference samples in the presence of r interfering target returns (given by Eq. (33)), the above equation can be written as

$$\begin{aligned} F_{Z_{MX}}(z) \ = \ & \sum_{i=K_1}^{N_1} \sum_{j=\max(0,i-r_1)}^{\min(i,N_1-r_1)} \left(\begin{array}{c} N_1 - r_1 \\ j \end{array} \right) \left(\begin{array}{c} r_1 \\ i-j \end{array} \right) \\ & \times \sum_{k=0}^{j} \sum_{\ell=0}^{i-j} \left(\begin{array}{c} j \\ k \end{array} \right) \left(\begin{array}{c} i-j \\ \ell \end{array} \right) (-1)^{i-k-\ell} \\ & \times \left\{ \sum_{m=0}^{M-1} \frac{\left(\frac{z}{\psi}\right)^m}{\Gamma(m+1)} e^{-\frac{z}{\psi}} \right\}^{N_1-r_1-k} \\ & \times \left\{ \sum_{n=1}^{M} b_n e^{-c_n z} \right\}^{r_1-\ell} F_{K_2}(z; N_2, r_2) \end{aligned} \tag{43}$$

By taking the Laplace transformation for the above equation, we obtain

$$\Phi_{F_{Z_{MX}}}(\omega) = \sum_{i=K_1}^{N_1} \sum_{j=\max(0,i-r_1)}^{\min(i,N_1-r_1)} \left(\begin{array}{c} N_1 - r_1 \\ j \end{array} \right) \left(\begin{array}{c} r_1 \\ i-j \end{array} \right)$$

$$\times\sum_{k=0}^{j}\sum_{\ell=0}^{i-j}\binom{j}{k}\binom{i-j}{\ell}(-1)^{i-k-\ell}\sum_{\theta_0=0}^{N_1-r_1-k}\sum_{\theta_1=0}^{N_1-r_1-k}$$
$$\cdots\sum_{\theta_{M-1}=0}^{N_1-r_1-k}\frac{\Omega(N_1-r_1-k;\theta_0,\ldots,\theta_{M-1})}{\prod_{v=0}^{M-1}[\Gamma(v+1)]^{\theta_v}}\left(\frac{1}{\psi}\right)^{\sum_{\eta=0}^{M-1}\eta\theta_\eta}$$
$$\times\sum_{\vartheta_1=0}^{r_1-\ell}\sum_{\vartheta_2=0}^{r_1-\ell}\cdots\sum_{\vartheta_M=0}^{r_1-\ell}\Omega(r_1-\ell;\vartheta_1,\ldots,\vartheta_M)\prod_{\xi=1}^{M}(b_\xi)^{\vartheta_\xi}$$
$$\times(-1)^{\sum_{\gamma=0}^{M-1}\gamma\theta}\frac{d^{\sum_{\gamma=0}^{M-1}\gamma\theta_\gamma}}{d\omega^{\sum_{\gamma=0}^{M-1}\gamma\theta_\gamma}}\{\Phi_{F_{K_2}}(\omega;N_2,r_2)\}\Big|_{\omega=\omega+\frac{N_1-r_1-k}{\psi}+\sum_{\zeta=1}^{M}\vartheta_\zeta c_\zeta} \tag{44}$$

where

$$(-1)^m\frac{d^m}{d\omega^m}\{\Phi_{F_{K_2}}(\omega;N_2,r_2)\}=\sum_{i=K_2}^{N_2}\sum_{j=\max(0,i-r_2)}^{\min(i,N_2-r_2)}\binom{N_2-r_2}{j}\binom{r_2}{i-j}$$
$$\times\sum_{k=0}^{j}\sum_{\ell=0}^{i-j}\binom{j}{k}\binom{i-j}{\ell}(-1)^{i-k-\ell}\sum_{\theta_0=0}^{N_2-r_2-k}\sum_{\theta_1=0}^{N_2-r_2-k}$$
$$\cdots\sum_{\theta_{M-1}=0}^{N_2-r_2-k}\frac{\Omega(N_2-r_2-k;\theta_0,\ldots,\theta_{M-1})}{\prod_{v=0}^{M-1}[\Gamma(v+1)]^{\theta_v}}\left(\frac{1}{\psi}\right)^{\sum_{\eta=0}^{M-1}\eta\theta_\eta}$$
$$\times\sum_{\vartheta_1=0}^{r_2-\ell}\sum_{\vartheta_2=0}^{r_2-\ell}\cdots\sum_{\vartheta_M=0}^{r_2-\ell}\Omega(r_2-\ell;\vartheta_1,\ldots,\vartheta_M)\prod_{\xi=1}^{M}(b_\xi)^{\vartheta_\xi}$$
$$\times\frac{\Gamma\left(\sum_{\gamma=0}^{M-1}\gamma\theta_\gamma+m+1\right)}{\left(\omega+\frac{N_2-r_2-k}{\psi}+\sum_{\zeta=1}^{M}\vartheta_\zeta c_\zeta\right)^{\sum_{\gamma=0}^{M-1}\gamma\theta_\gamma+m+1}} \tag{45}$$

Once the Laplace transformation of the CDF of the final noise power level estimate is calculated, the MGF and consequently the processor

performance is completely determined. Consequently, the false alarm and detection probabilities of the MX-OS processor can be easily evaluated since the MGF of the noise power level estimate is the backbone of their expressions.

3.2.3. Minimum (MN)-OS Detector

The minimum operation has been introduced to alleviate the problems associated with closely spaced targets leading to two or more targets appearing in the reference window. While testing for target presence at a particular range, the processor must not be influenced by the extraneous target echoes. It has been shown that although the MN-OS detector exhibits greater additional detectability loss in homogeneous environments (relative to the other modified versions), it does perform well in multiple target environment when a cluster of radar targets appears in the reference windows.

The MN operation is capable of resolving multiple targets in the reference window as long as all the interferers appear either in the leading or lagging window. However, this scheme has undesired effects when interfering targets are located in both halves of the reference window and their number is outside their allowable range [11].

In this type of CFAR schemes, the noise power level is estimated by taking the minimum of the local noise level estimates Z_1 and Z_2 as depicted in Fig. 1. That is

$$Z_{MN} = \min(Z_1, Z_2) \tag{46}$$

In this case, the noise power level estimate has a PDF given by [7]

$$f_{Z_{MN}}(z) = f_{Z_1}(z) + f_{Z_2}(z) - f_{Z_{MX}}(z) \tag{47}$$

The last term in the above expression is simply the PDF of Z_{MX} for the MX-OS. All the PDF terms in the right hand side of the above expression are previously determined and consequently the statistic of the noise level estimate Z_{MN} is completely known. The Laplace transformation of Eq. (47) yields

$$M_{Z_{MN}}(\omega) = M_{Z_1}(\omega) + M_{Z_2}(\omega) - M_{Z_{MX}}(\omega) \tag{48}$$

The expression (48) gives a very simple relationship between the performance of MN-OS and that of MX-OS detection performance. Again, we state that once the MGF of the noise power level estimate is calculated, the processor false alarm and detection performances are fully determined. Finally, a desirable CFAR scheme would of course be one that is insensitive to changes in the total noise power within the reference window cells so that a constant false alarm rate is maintained.

4. PROCESSOR PERFORMANCE ASSESSMENT

To illustrate the performance of CFAR processors for partially correlated χ^2 fluctuating targets, the previous analytical expressions are programmed on a digital computer for some parameter values and the results of these programs are presented, for OSD(21), ML-OSD(10), MX-OSD(10) and MN-OSD(10) in Figs. 2–5, respectively. The abbreviation OSD(21) means the single-window OS detector with ordered-statistic parameter K of 21, while the other three abbreviations denote double-window OS detectors with symmetrical ordered-statistic parameter values of 10 ($K_1 = K_2 = 10$). The reference window size (N) is chosen to be 24, the design P_{fa} is 10-6 and two values (2 & 4) for the number of integrated pulses are selected. For comparison, these figures also include the single sweep processor detection performance, relative to which we can demonstrate the processor performance improvement for $M > 1$. Besides the single sweep curve, there are another two families of curves. The first family indicates the detection performance of the processor under consideration for partially correlated χ^2 targets (with $\rho_s = 0$, 0.5, 0.9 and 1) when the number of integrated pulses is two ($M = 2$). The curves of this set are labeled in the signal correlation coefficient ρ_s, including the SWII fluctuation model ($\rho_s = 0$) and the SWI model ($\rho_s = 1$), and the number of integrated pulses M. Examining the

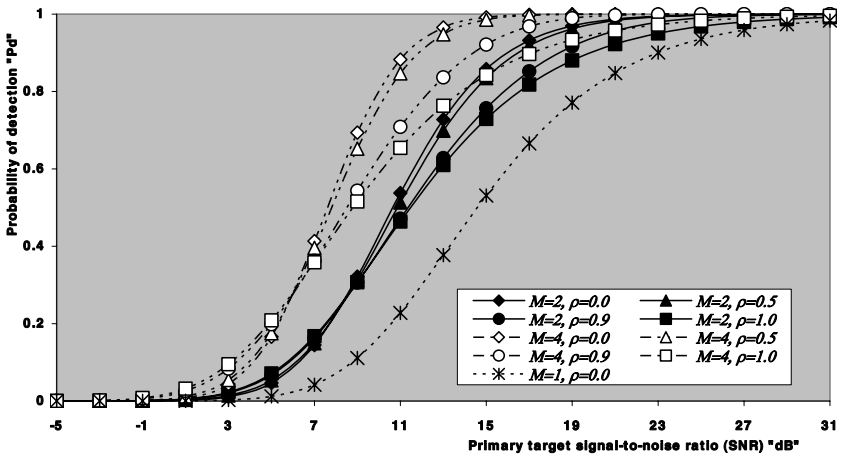

Figure 2. M-sweeps homogeneous detection performance of OSD(21) for partially correlated chi-square fluctuating targets with two-degrees of freedom when $N = 24$, and $P_{fa} = 1.0$E-6.

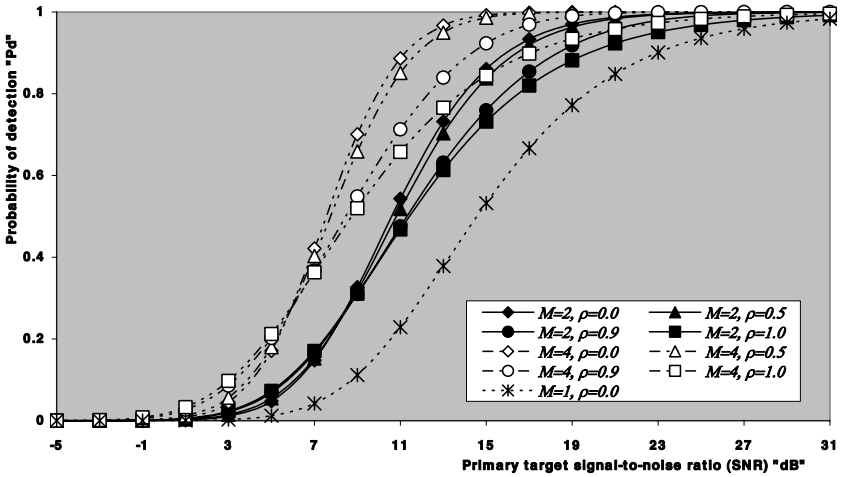

Figure 3. M-sweeps homogeneous detection performance of ML-OS(10) for partially correlated chi-square fluctuating targets with two-degrees of freedom when $N = 24$, and $P_{fa} = 1.0\text{E-}6$.

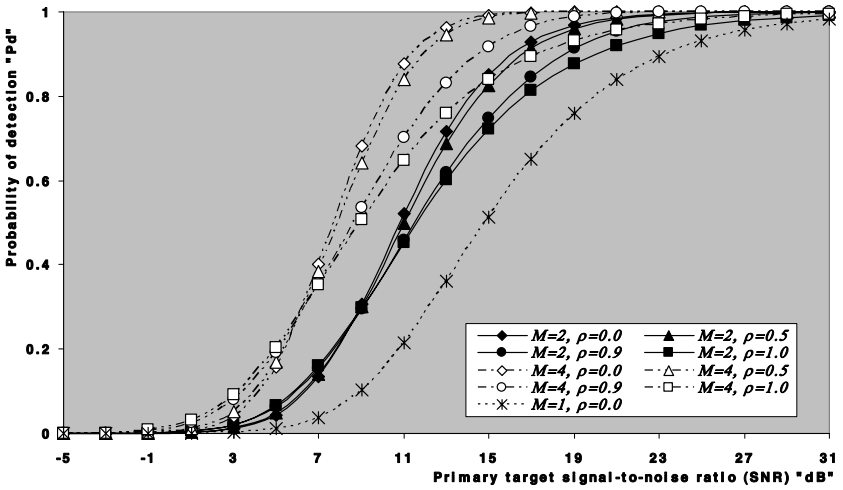

Figure 4. M-sweeps homogeneous detection performance of MX-OS(10) for partially correlated chi-square fluctuating targets with two-degrees of freedom when $N = 24$, and $P_{fa} = 1.0\text{E-}6$.

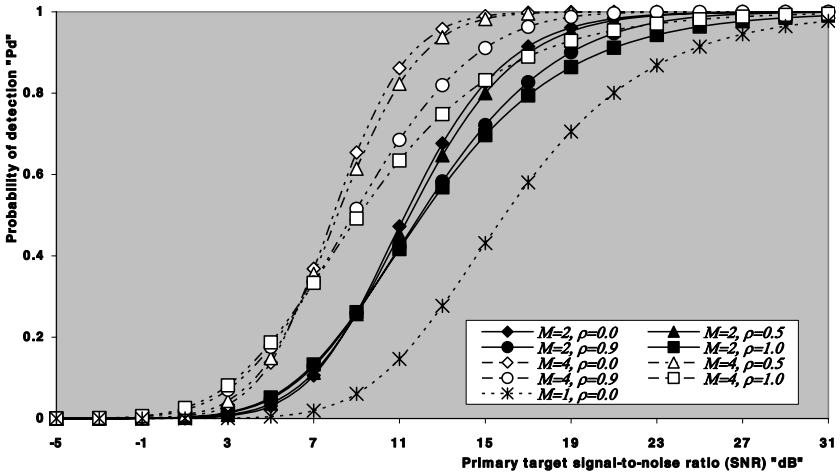

Figure 5. M-sweeps homogeneous detection performance of MN-OS(10) for partially correlated chi-square fluctuating targets with two-degrees of freedom when $N = 24$, and $P_{fa} = 1.0\text{E-}6$.

candidates of this group of curves, we observe that as ρ_s increases from zero to unity, more per pulse average SNR is required to achieve the same probability of detection. The second group includes the processor detection performance for partially correlated χ^2 targets (with the same ρ_s values as above) when the number of postdetection integrated pulses is four ($M = 4$). Examining the candidates of the two families, we note that for low SNR, P_d increases monotonically with ρ_s, while P_d degrades as ρ_s increases when the strength of the target return (SNR) is high. In addition, for fixed SNR, the processor performance improves with increasing M. However, the degradation in P_d increases with increasing ρ_s. This is common for the four detectors considered in this manuscript.

The nonhomogeneous performances of these processors are evaluated for a maximum allowable number of extraneous targets in each reference window. If K is chosen to be 21, for single-window detector, then the processor is able to discriminate the primary target from, at most, three outlying targets with little degradation in detection performance. For double-window processor, on the other hand, the ordered-statistic parameter K is chosen to be 10. As a result of this, the processor is able to discriminate the primary target from two extraneous targets. Therefore, the double-window processor detection performance is evaluated for $r_1 = N_1 - K_1 = 2$ and $r_2 = N_2 - K_2 = 2$. Our results are obtained for a possible practical

situation where the primary and the secondary interfering targets fluctuate in accordance with the χ^2 fluctuation model with the same correlation coefficient ($\rho_s = \rho_i$) and of equal target return strength (INR=SNR). Figs. 6–9 illustrate the multiple-target performance of OSD(21), ML-OSD(10), MX-OSD(10) and MN-OSD(10), respectively. As in homogeneous case, the reference window size (N) is chosen to be 24, the design P_{fa} is 10^{-6} and two values (2 & 4) for the number of integrated pulses are selected. For comparison, these figures also include the single sweep processor detection performance, relative to which we can demonstrate the processor performance improvement for $M > 1$. Besides the monopulse curve, there are another two families of curves. These families indicate the detection performance of the considered algorithm for partially correlated χ^2 targets (with $\rho_s = 0$, 0.5, 0.9 and 1) when the number of integrated pulses is 2 and 4, respectively. Their curves are labeled in the signal correlation coefficient ρ_s, including the SWII fluctuation model ($\rho_s = 0$) and the SWI model ($\rho_s = 1$), and the number of integrated pulses M. Examining the curves of this category, leads us to conclude that the behavior of the processor under consideration in the presence of extraneous targets is the same as its behavior in the absence of them with only minor degradation. In addition, as ρ_s increases from zero to unity, more per pulse average SNR is required to achieve the same probability of detection.

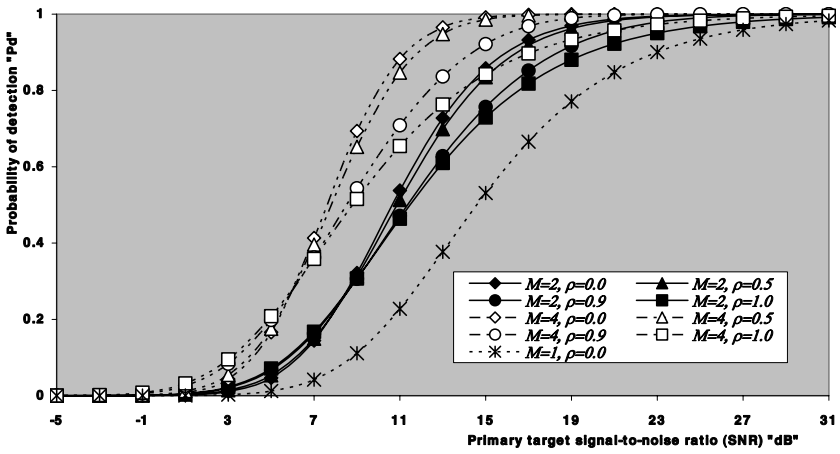

Figure 6. M-sweeps multitarget detection performance of OSD(21) scheme for partially correlated chi-square fluctuating targets with two-degrees of freedom when $N = 24$, $R = 3$, and $P_{fa} = 1.0\text{E-}6$.

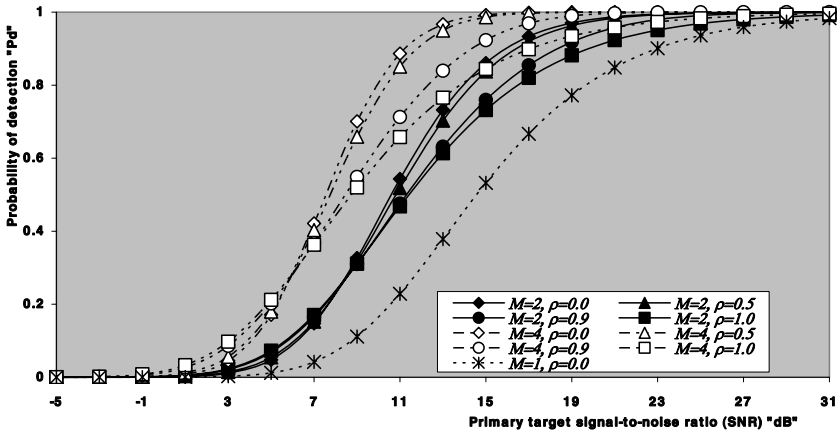

Figure 7. M-sweeps multitarget detection performance of ML-OS(10) scheme for partially correlated chi-square fluctuating targets with two-degrees of freedom when $N = 24$, $R_1 = R_2 = 2$, and $P_{fa} = 1.0\text{E-}6$.

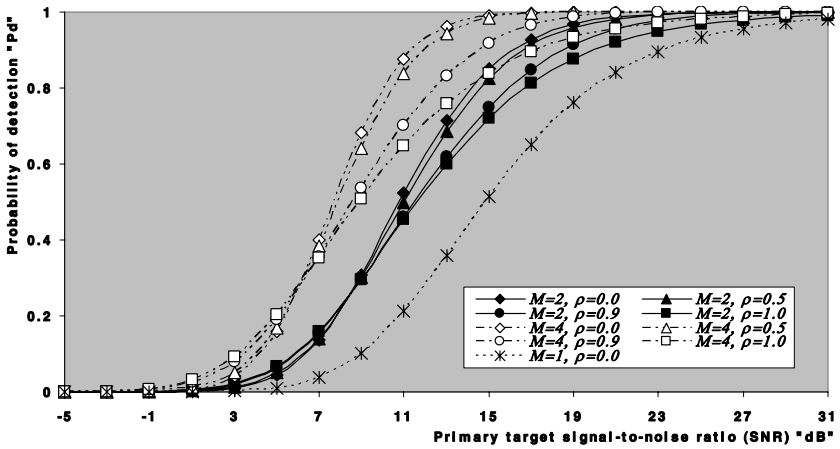

Figure 8. M-sweeps multitarget detection performance of MX-OS(10) scheme for partially correlated chi-square fluctuating targets w ith two-degrees of freedom when $N = 24$, $R_1 = R_2 = 2$, and $P_{fa} = 1.0\text{E-}6$.

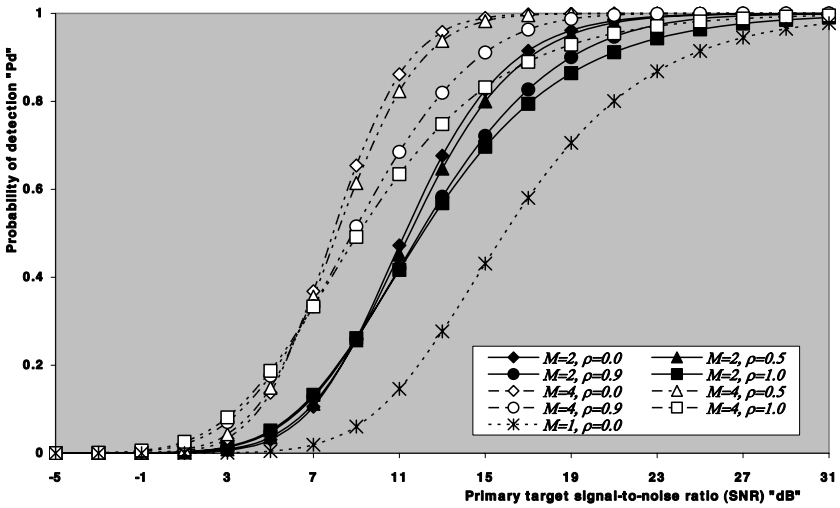

Figure 9. M-sweeps multitarget detection performance of MN-OS(10) scheme for partially correlated chi-square fluctuating targets with two-degrees of freedom when $N = 24$, $R_1 = R_2 = 2$, and $P_{fa} = 1.0\text{E-}6$.

In order to demonstrate the ability of the MN-OSD in resolving multiple targets, we have assumed that all the extraneous targets are located in the lagging window only ($r_1 = 0,\ r_2 = 4$). Fig. 10 shows the detection performance of different OS schemes under this condition for SWI & SWII fluctuation models. The curves of these figures are labeled in the detector under consideration and the fluctuation model when $M = 3$. From these results, we observe that intolerable masking of the primary target occurs in the case of OS(21), ML- and MX-OSD(10), and the masking effect is greater in the MX than in the ML scheme. The MN is the only scheme that is capable of resolving multiple targets in the reference window as long as all the interferers appear in either one of the local windows.

The variation of the false alarm rate with the strength of the interfering targets, when these targets are located in only one of the local windows, is shown in Fig. 11 for $M = 3$. This figure illustrates the superiority of the MN scheme in maintaining a constant rate of false alarm when it is operated in multiple-target environments when the extraneous targets fluctuate following either SWI or SWII model. The next processor is the single-window scheme then comes the modified version ML and finally the MX operation has the worst performance in maintaining a constant rate of false alarm in multtarget environment. In addition, the false alarm rate performance of these detectors is

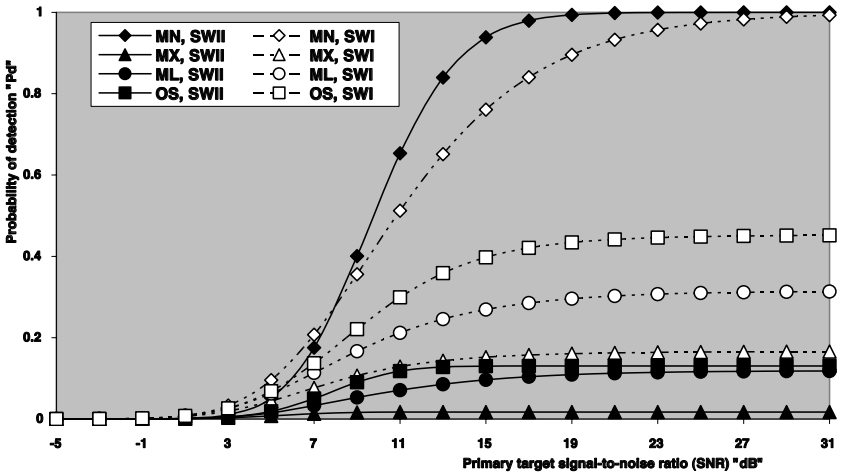

Figure 10. Multitarget detection performance of OS family of CFAR schemes for chi-square fluctuating targets with two-degrees of freedom when $N = 24,\ M = 3,\ R = 4,\ R_1 = 0,\ R_2 = 4$, and $P_{fa} = 1.0\text{E-}6$.

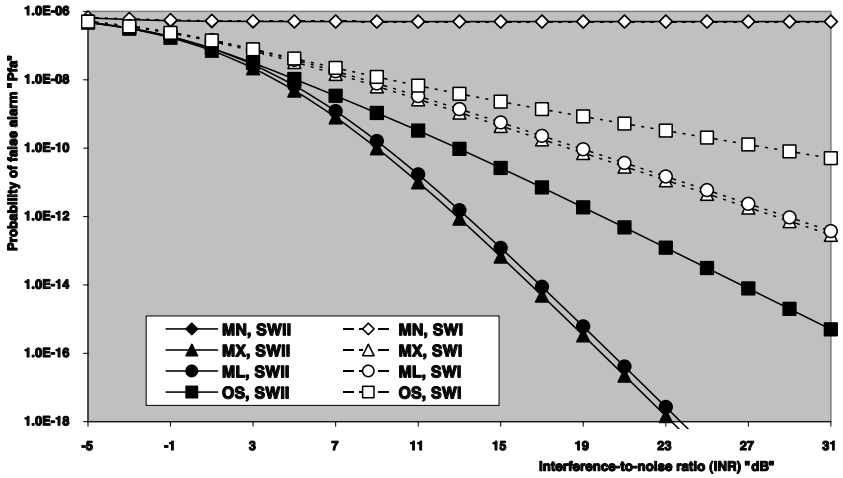

Figure 11. False alarm rate performance of OS based detectors for chi-square fluctuating targets with two-degrees of freedom when $N = 24,\ M = 3,\ R = 4,\ R_1 = 0,\ R_2 = 4$, and design $P_{fa} = 1.0\text{E-}6$.

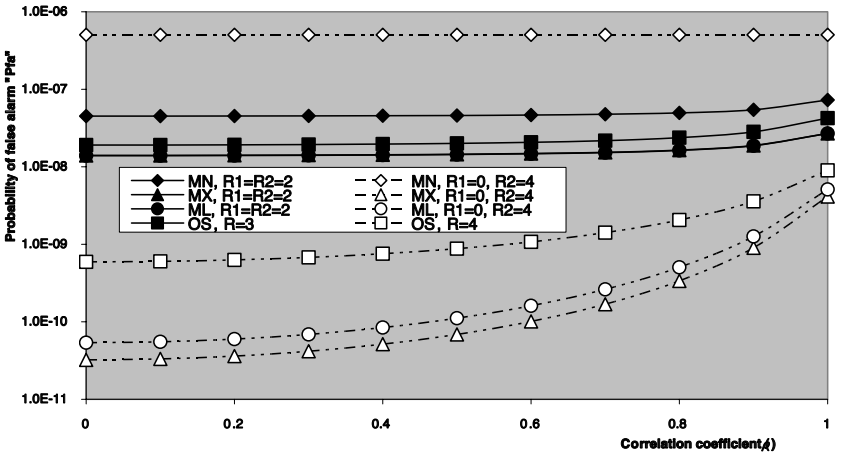

Figure 12. Multitarget false alarm rate performance of OS family of CFAR schemes for partially correlated chi-square fluctuating targets when $N = 24,\ M = 3,\ INR = 10\,\text{dB}$, and design $P_{fa} = 1.0\text{E-}6$.

higher for SWI fluctuation model than their performance when the outlying targets fluctuate following SWII model. Fig. 12 depict the false alarm rate performance of the OS based detectors as a function of consecutive sweeps correlation coefficient for an interfering target strength of 10 dB and $M = 3$, when the spurious target returns are contained in both reference windows ($r_1 = r_2 = 2$) and in the case where only one of the reference windows is contaminated interfering target returns ($r_1 = 0$ & $r_2 = 4$). The results of this figure demonstrate our previous conclusion. In addition, the false alarm rate behavior of the OS modified versions in the case where both reference windows contaminated with interfering target returns is higher than their performance when only one of these windows is contaminated with these undesired returns. The MN-OS technique is the only one which don't follow this rule in its reaction against outlying target returns if the desired false alarm rate is required to be constant. Moreover, the processor performance improves as the correlation coefficient among consecutive sweeps increases. Fig. 13 illustrates the required SNR for the OS based detectors to achieve an operating point of $(10^{-6}, P_d)$, as a function of the detection probability P_d, when the radar receiver operates in homogeneous and multiple-target environments. As a reference of comparison, this figure depicts also the same behavior for the optimum detector. From the results of this figure, we observe that the ML-OS requires the lowest, relative to

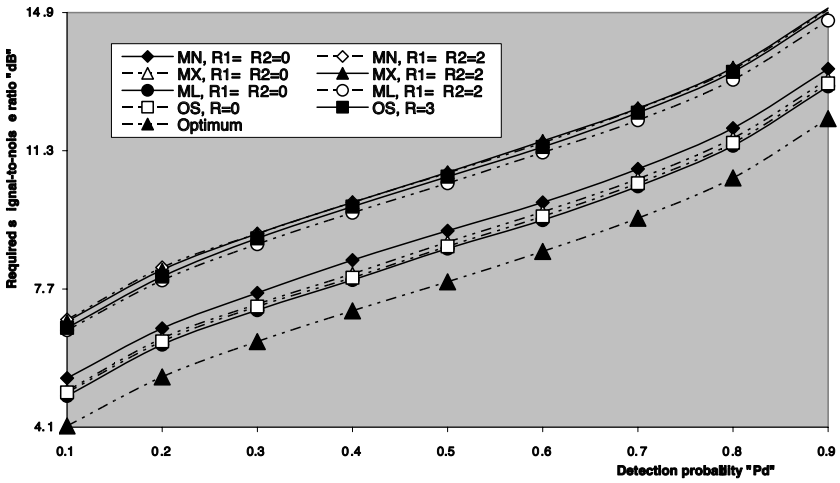

Figure 13. Homogeneous and multitarget required SNR to achieve an operating point (P_{fa}, P_d) of OS based schemes for fluctuating targets of SWII model when $N = 24,\ M = 3$, and $P_{fa} = 1.0\text{E-}6$.

other candidates in its category, SNR to achieve a specified value for P_d and the MN-OS needs the largest value of SNR to attain the same value of P_d. As a conformation of this statement, Fig. 14 shows the required SNR to attain a given operating point of (10^{-6}, 0.9) as a function of the ranking-order parameter K, for the OS based detectors, along with the fixed threshold processor, when the radar receiver operates in an ideal environment and integrates 3 consecutive sweeps in its signal processing. Finally, the required SNR, in homogeneous as well as in multiple-target environments, against the correlation coefficient is drawn in Fig. 15) for the OS based algorithms along with the optimum scheme when the radar receiver postdetection integrates 3-pulses. The curves of this figure are labeled in the CFAR scheme, r_1 and r_2. The numerical results of this figure are given for a maximum allowable number of extraneous targets in each case. This figure illustrates that the processor detection performance degrades with ρ and that the processor performance for SWII is higher than its performance for SWI target fluctuation models. The ML scheme has the best detection performance either in the absence or in the presence of spurious targets given that their number is within the allowable range.

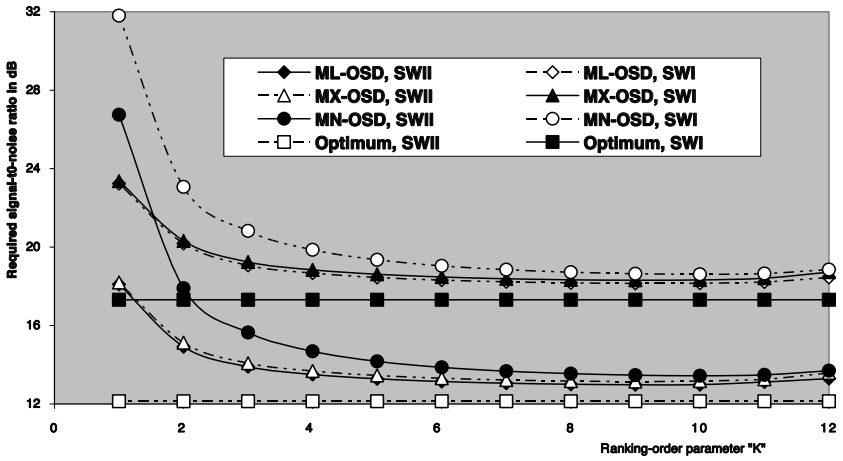

Figure 14. Required SNR to achieve an operating point (1.0E-6, 0.9) of OS based schemes for SWI and SWII target fluctuation models, in ideal environment, when $N = 24$ and $M = 3$.

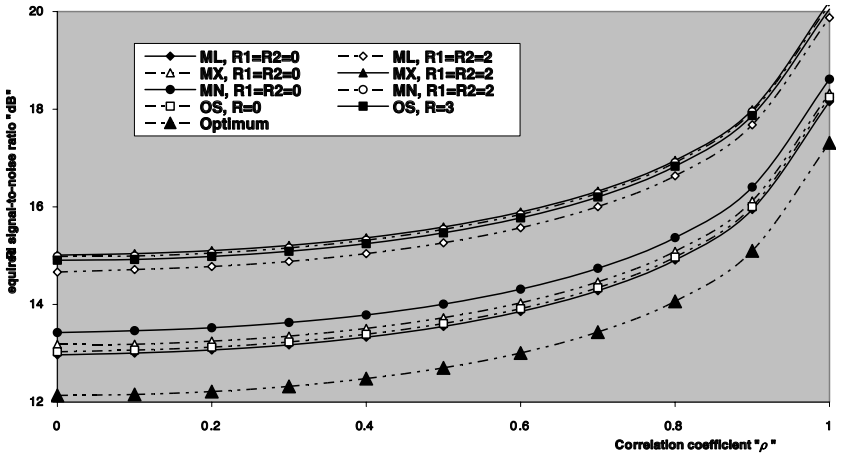

Figure 15. Homogeneous and multitarget required SNR to achieve an operating point (1.0E-6, 0.9) of OS based schemes for partially correlated chi-square fluctuating targets when $N = 24$ and $M = 3$.

5. CONCLUSIONS

The problem of detecting radar targets against a background of unwanted clutter and noise is studied. We have derived exact detection probabilities for CFAR processors based, in their local noise power level estimation, on the ordered-statistic technique for partially correlated χ^2 targets. These processors include the conventional OS detector along with its modified versions which include ML-, MX- and MN-OS algorithms for their performance evaluation in the absence as well as in the presence of spurious targets. The primary and secondary interfering targets are assumed to be fluctuating in accordance with the χ^2 fluctuation model with two degrees of freedom. At the limiting correlation coefficients $\rho = 1$ and $\rho = 0$, the analysis yields, respectively, the well known SWI and SWII models. The results are given in a closed form expressions with especially simple form for a SW II fluctuation model. The analytical results have been used to develop a complete set of performance curves including the detection probability in homogeneous and multiple target situations, the variation of false alarm rate with the strength of interfering targets that may exist amongst the contents of the estimation set, and the required SNR to achieve a prescribed operating point (P_{fa}, P_d), as a function of the ordered-statistic parameter and correlation coefficient. As expected, lower threshold values and consequently higher detection performance is obtained as the number of postdetection integrated pulses increases. On the other hand, as the signal correlation increases from zero to unity, more per pulse SNR is required to achieve a prescribed probability of detection. In addition, the false alarm rate increases with the signal correlation and the MN-OS scheme is the only processor that is capable of maintaining a constant rate of false alarm, irrespective to the interference level, in the case where the spurious targets are located in either one of the reference windows.

The tradeoffs to be compromised, concerning selection of the appropriate type of processor and an adequate choice of the reference window size, are manifold and highly dependent on the specific clutter and interference models assumed, in particular in a nonhomogeneous environment. Therefore, an optimal and general purpose CFAR detector can almost never be devised. When the size of the reference window is increased, the CFAR loss in a stationary noise background monotonically decreases to zero, together with an increased hardware complexity, and an inevitable violation of the inherent assumption that the noise samples are identically distributed over the reference cells and properly represent the noise level in the detection cell. Therefore, in a nonhomogeneous environment, the CFAR penalty sometimes increases

with increasing the reference window size. In addition, the likelihood that an interfering target or a spiky clutter return has entered the reference window is obviously larger for larger number of reference cells. On the other hand, once the window has been captured by an interfering target, the primary target is less suppressed when the size of the reference window is large.

When the target signal fluctuates obeying χ^2 statistics, the signal components are correlated from pulse to pulse and this correlation degrades the processor performance. A common and accepted practice in radar system design to mitigate the effect of target fluctuation is to provide frequency diversity to decorrelate the signal from pulse to pulse. While this technique is effective, it requires additional system complexity and cost.

REFERENCES

1. Dillard, G. M., "Mean level detection of nonfluctuating signals," *IEEE Transactions on Aerospace and Electronic Systems*, Vol. AES-10, 795–799, Nov. 1974.
2. Rickard, J. T. and G. M. Dillard, "Adaptive detection algorithm for multiple target situations," *IEEE Transactions on Aerospace and Electronic Systems*, Vol. AES-13, 338–343, July 1977.
3. Nitzberg, R., "Analysis of the arithmetic mean CFAR normalizer for fluctuating targets," *IEEE Transactions on Aerospace and Electronic Systems*, Vol. AES-10, 44–47, Jan. 1978.
4. El Mashade, M. B., "M-sweeps exact performance analysis of OS modified versions in nonhomogeneous environments," *IEICE Trans. Commun.*, Vol. E88-B, No. 7, 2918–2927, July 2005.
5. Rohling, H., "Radar CFAR thresholding in clutter and multiple target situations," *IEEE Transactions on Aerospace and Electronic Systems*, Vol. AES-19, 608–621, July 1983.
6. Kanter, I., "Exact detection probability for partially correlated Rayleigh targets," *IEEE Transactions on Aerospace and Electronic Systems*, Vol. AES-22, 184–196, Mar. 1986.
7. Gandhi, P. P. and S. A. Kassam, "Analysis of CFAR processors in nonhomogeneous backgrounds," *IEEE Transactions on Aerospace and Electronic Systems*, Vol. AES-24, 427–445, July 1988.
8. Elias-Fuste, A. R., M. G. De Mercado, and E. R. Davo, "Analysis of some modified ordered-statistic CFAR: OSGO and OSSO CFAR," *IEEE Transactions on Aerospace and Electronic Systems*, Vol. AES-26, 197–202, January 1990.
9. Lim, C. H. and H. S. Lee, "Performance of order-statistics

CFAR detector with noncoherent integration in homogeneous situations," *IEE Proceedings-F*, Vol. 140, No. 5, 291–296, October 1993.

10. He, Y., "Performance of some generalized modified order-statistics CFAR detectors with automatic censoring technique in multiple target situations," *IEE Proc. - Radar, Sonar Navig.*, Vol. 141, No. 4, 205–212, August 1994.
11. El Mashade, M. B., "Performance analysis of modified ordered statistics CFAR processors in nonhomogeneous environments," *Signal Processing "ELSEVIER"*, Vol. 41, 379–389, Feb. 1995.
12. Swerling, P., "Radar probability of detection for some additional fluctuating target cases," *IEEE Transactions on Aerospace and Electronic Systems*, Vol. AES-33, 698–709, April 1997.
13. El Mashade, M. B., "Performance analysis of OS family of CFAR schemes with incoherent integration of M-pulses in the presence of interferers," *IEE Radar, Sonar Navig.*, Vol. 145, No. 3, 181–190, June 1998.
14. El Mashade, M. B., "Analysis of adaptive radar systems processing M-sweeps in target multiplicity and clutter boundary environments," *Signal Processing "ELSEVIER"*, Vol. 67, 307–329, Aug. 1998.
15. El Mashade, M. B., "Target multiplicity performance analysis of radar CFAR detection techniques for partially correlated chi-square targets," *Int. J. Electron. Commun. AEÜ*, Vol. 56, No. 2, 84–98, April 2002.
16. El Mashade, M. B., "Analysis of cell-averaging based detectors for χ^2 fluctuating targets in multitarget environments," *Journal of Electronics China*, Vol. 23, No. 6, 853–863, November 2006.